Polymer Testing 29 (2010) 544–552

Contents lists available at ScienceDirect

Polymer Testing

journal homepage: www.elsevier.com/locate/polytest

Test Method

# Thermomechanical characterization of shape memory polymers using high temperature nanoindentation

J.T. Fulcher [a], Y.C. Lu [a,*], G.P. Tandon [b,c], D.C. Foster [b]

[a] University of Kentucky, Lexington, KY 40506, USA
[b] Air Force Research Laboratory, Materials and Manufacturing Directorate, AFRL/RXBC, Wright-Patterson AFB, OH 45433, USA
[c] University of Dayton Research Ins., 300 College Park, Dayton, OH 45469-0060, USA

ARTICLE INFO

*Article history:*
Received 20 December 2009
Accepted 1 February 2010

*Keywords:*
Shape memory polymer
High temperature nanoindentation
Thermomechanical characterization
Shape recovery

ABSTRACT

This paper investigates the thermomechanical behavior of a thermosetting shape memory polymer (SMP) by using a high temperature nanoindentation technique. The nanoindenter is equipped with a microheater and a sophisticated temperature control and monitoring system. This allows the SMP to be activated at elevated temperatures enabling proper implementation of the thermomechanical cycle typically used to quantify the shape memory behavior. The load–depth curves of the SMP were obtained at various temperatures, from which the instantaneous moduli were calculated with a revised indenter-sample contact depth formula. The moduli from nanoindentation are consistent with those obtained from dynamic mechanical analysis on bulk samples. When activated at elevated temperatures, the SMP exhibits surface profiles different from those obtained when activated at room temperature. A large amount of "sink-in" is observed at the SMP surface when activated at temperatures above its glass transition temperature ($T_g$). It is seen that the large-strain elastic deformation is almost fully recoverable when recovery takes place at a recovery temperature, $T_r > T_g$.



## 1. Introduction

Shape-memory polymers (SMP) are an emerging class of active polymers that can be used in a broad range of applications in deployable aerospace structures, biomedical devices, and microsystems [1–7]. SMP have the ability to change shape in a predefined way from a temporary shape to a permanent shape when exposed to an appropriate stimulus. The temporary shape is obtained by mechanical deformation and subsequent fixation of that deformation. Upon application of an external stimulus, the polymer recovers its initial shape. This cycle of programming and recovery can be repeated several times [8], with different temporary shapes in subsequent cycles. Compared with shape-memory alloys, shape-memory polymers possess the advantages of high elastic deformation, low cost, low density, and potential biocompatibility and biodegradability.

The external stimulus for actuation of SMP is often thermal. The typical thermomechanical cycles used to quantify the shape-memory behavior of the SMP have been described by Lendlein and Kelch [1], Liu et al. [3,4], Gall et al. [9], Tobushi et al. [10,11], and Atli et al. [12]. A schematic representation of the thermomechanical cycle of a SMP is illustrated in Fig. 1. First, the SMP is activated at the deformation temperature, $T_d$, which should be above the material's glass transition temperature, $T_g$. Secondly, the constrained SMP is cooled to the storage temperature, $T_s$, which is below $T_g$. Finally, the SMP is heated up again to a recovery temperature, $T_r$, to allow the shape to recover freely. The recovery temperature may be a range of temperatures at which the SMP recovers its initial permanent shape during heating.

* Corresponding author.
*E-mail address:* chlu@engr.uky.edu (Y.C. Lu).

0142-9418/$ – see front matter © 2010 Elsevier Ltd. All rights reserved.
doi:10.1016/j.polymertesting.2010.02.001

# Report Documentation Page

*Form Approved*
*OMB No. 0704-0188*



| 1. REPORT DATE | 2. REPORT TYPE | 3. DATES COVERED |
|---|---|---|
| **2010** | | **00-00-2010 to 00-00-2010** |

| 4. TITLE AND SUBTITLE | 5a. CONTRACT NUMBER |
|---|---|
| **Thermomechanical characterization of shape memory polymers using high temperature nanoindentation** | 5b. GRANT NUMBER |
| | 5c. PROGRAM ELEMENT NUMBER |
| 6. AUTHOR(S) | 5d. PROJECT NUMBER |
| | 5e. TASK NUMBER |
| | 5f. WORK UNIT NUMBER |
| 7. PERFORMING ORGANIZATION NAME(S) AND ADDRESS(ES) **University of Kentucky,Lexington,KY,40506** | 8. PERFORMING ORGANIZATION REPORT NUMBER |
| 9. SPONSORING/MONITORING AGENCY NAME(S) AND ADDRESS(ES) | 10. SPONSOR/MONITOR'S ACRONYM(S) |
| | 11. SPONSOR/MONITOR'S REPORT NUMBER(S) |

12. DISTRIBUTION/AVAILABILITY STATEMENT
**Approved for public release; distribution unlimited**

13. SUPPLEMENTARY NOTES

14. ABSTRACT

15. SUBJECT TERMS

| 16. SECURITY CLASSIFICATION OF: | | | 17. LIMITATION OF ABSTRACT | 18. NUMBER OF PAGES | 19a. NAME OF RESPONSIBLE PERSON |
|---|---|---|---|---|---|
| a. REPORT | b. ABSTRACT | c. THIS PAGE | | | |
| **unclassified** | **unclassified** | **unclassified** | **Same as Report (SAR)** | **9** | |

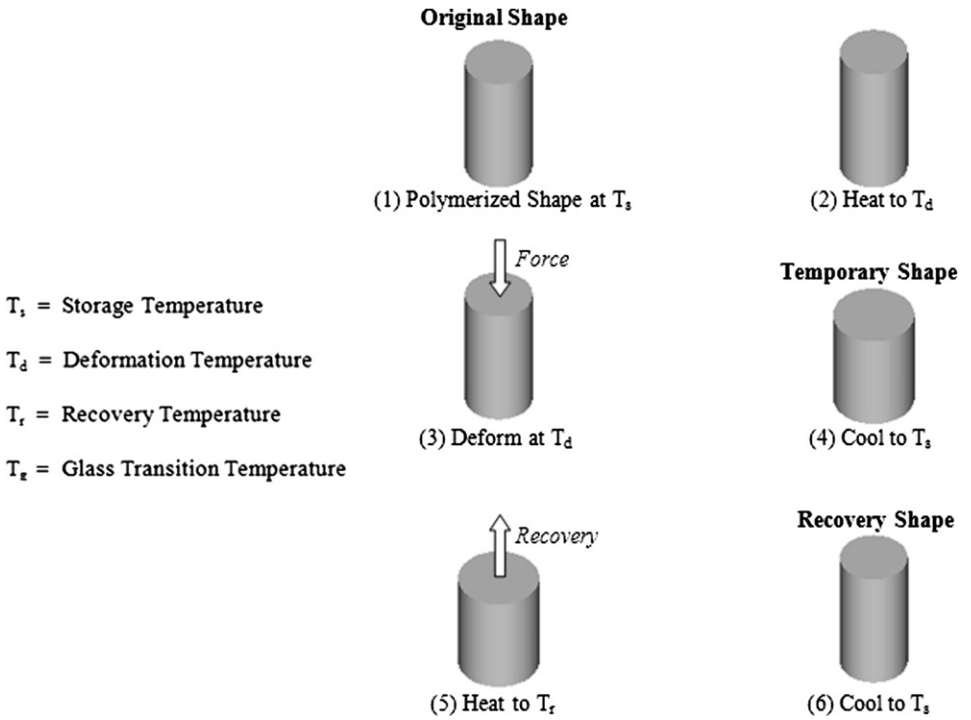


**Fig. 1.** Schematic of the shape memory cycle test for shape memory polymers (SMP).

Recently, the shape memory effect of SMP on a small scale has been increasingly studied, mostly through the micro-/nano-indentation technique [9,13–15]. However, the thermal–mechanical indentations have been performed at ambient temperature (below the material's glass transition temperature). The deformed specimens are then heated to above $T_g$ through an additional heating source and the shape recovery effects are examined. It is noted that such tests are inconsistent with the correct thermo-mechanical cycle as illustrated in Fig. 1. Although it is arguable that the SMP may be activated at temperatures lower than $T_g$, in doing so the true shape memory process of the materials may not be fully revealed.

As a well established method for characterizing the deformation of materials and structure on a small scale, nanoindentation is still somewhat limited to measuring the mechanical properties at ambient temperature. Only a relatively small amount of literature is available addressing the use of high temperature nanoindentation. Schuh et al. [16] has recently conducted a comprehensive study on high temperature nanoindentation on fused silica. The purpose of that work was mainly to quantify the thermal stability of the indentation equipment. Beake and Smith [17] have reported high temperature nano-indentation experiments on fused silica and soda–lime glass. Volinsky et al. [18] and Sawant and Tin [19] have recently reported the uses of high temperature nano-indentation for characterizing the mechanical properties of hard thin films and single crystal super-alloys. We have recently used the high temperature nanoindenter to measure the mechanical properties of polymer resins at elevated temperatures [20]. In the present study, we use the high-temperature indentation technique to examine the thermomechanical and shape-recovery behavior of a thermosetting, epoxy-based SMP.

## 2. Experimental technique

### 2.1. Materials

The epoxy-based thermosetting SMP resin (VFE2-100), developed by Cornerstone Research Group, Inc. (CRG), was used in the present study. Rectangular neat resin plaques measuring 30 cm by 30 cm with an average thickness of 3.2 mm were fabricated using the manufacturer's suggested cure cycle (CRG data sheet [21]). Smaller specimens, 1 cm × 1 cm × 3.2 mm, were subsequently cut from the larger plates using a diamond saw with distilled water as a cooling media. For nanoindentation studies, the surface of the specimen was prepared by successive polishing, the final polishing compound being alumina with an average particle size of 0.3 μm. The specimens were then stored at room temperature for nanoindentation experiments.

### 2.2. High temperature nanoindenter

The high-temperature nanoindentation tests were performed on a Nano Indenter XP (MTS NanoInstruments, Oak Ridge, TN), equipped with a thermal management system (Fig. 2) consisting primarily of (a) a micro-heater sitting in an aluminum stage holder, (b) a stainless steel heat shield that was used to isolate the indenter transducer assembly from the heat source, (c) a coolant system that was used to remove heat from the surrounding stage, and

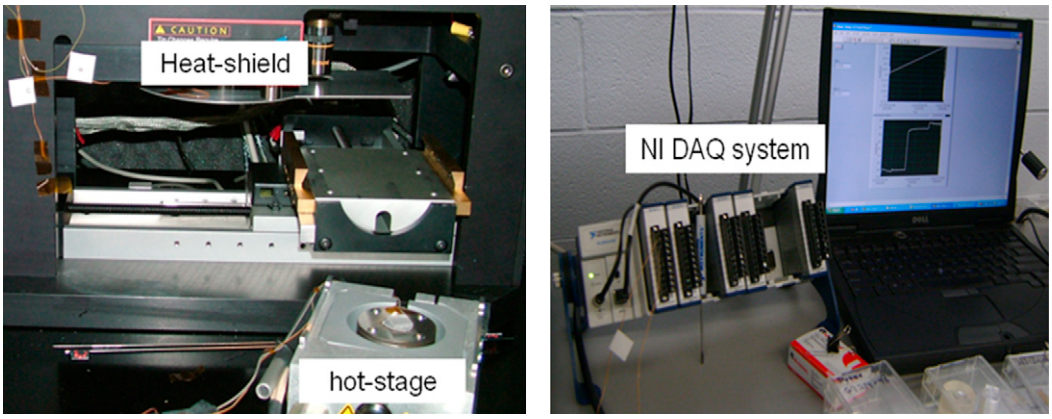


**Fig. 2.** High-temperature indentation apparatus used in the present experiments.

(d) a temperature control and monitoring system, operated through a NI (National Instrument) data acquisition device and LabView software. The temperatures of the sample, heater-stage and indenter frame were all monitored through multiple J-type thermocouples and the LabView data acquisition system. The SMP specimen was mounted on a special sample disk using a high-temperature adhesive (Poly-2000). This adhesive was designated for high temperature applications and has a low coefficient of thermal expansion. A spherical indenter with a tip radius of 100 μm was used in the present experiments. The latest tips provided by the manufacturer had all been brazed onto the tip holder, a process allowing tips to be used at elevated temperatures.

The thermal stability of the present nanoindenter frame was first determined by testing standard material, i.e., fused silica. The indentation load–depth curves of the fused silica were obtained at various temperatures: from ambient to 200 °C. There was negligible difference in load–depth responses in this range of temperatures. The modulus at each temperature was calculated from the load–depth curves following the standard Oliver–Pharr method [22,23] and results are shown in Fig. 3. The modulus of fused silica was observed to increase by a factor of approximately 1.02 as temperature was raised from ambient to 200 °C, which was consistent with the finding reported by Schuh et al. [16]. Thus, the present nanoindentation apparatus has negligible change in frame stiffness as the temperature increases and is, therefore, thermally stable.

### 2.3. Modulus measurement

The temperature-dependent modulus of the SMP was measured with the nanoindenter equipped with a micro-heater. Polymers exhibit time- and rate-dependent visco-elastic deformation, particularly at elevated temperatures. During the nanoindentation of a viscoelastic material, the resultant load–depth plot often exhibits a "bulge" in the initial unloading segment due to viscous creep, which would lead to errors in computing the correct contact stiffness ($S$). To minimize the creep effect (as well as other effects such as instrument drift) on the initial unloading set

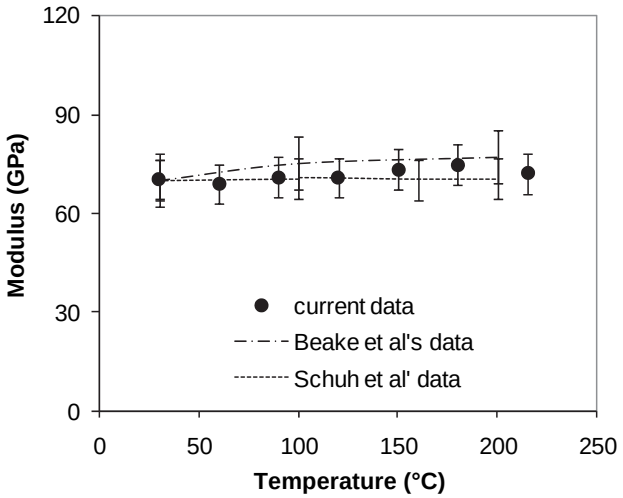


**Fig. 3.** Modulus of fused silica measured from the high temperature nanoindenters.

of data, the "hold-at-the-peak" method, as sketched in Fig. 4, has been typically used for testing polymeric materials [24–26]. In the present experiments, the indenter was loaded at a rate of 3.5 mN/s to a maximum load, and then held at the maximum load for a length of time (2 s–30 s) prior to starting unloading. With the addition of the indenter holding segment, the initial unloading curve no longer has the "bulge" so that the contact stiffness ($S$) can be computed following the standard Oliver–Pharr method [22,23].

### 2.4. Shape recovery ability tests

The shape memory behavior of the present SMP was examined using high temperature nanoindentation. The experiments were designed to ensure consistency with the standard shape memory cycle (as described in Fig. 1). First, the specimen was heated to a deformation temperature $T_d = 110\,^{\circ}C$ ($>T_g$). The heating rate was approximately 2 °C/min. The actual temperature in the specimen was monitored through thermocouples placed near the specimen. The specimen was kept at this temperature for at least 1-hr to allow the temperature in the specimen to reach equilibrium. The specimen was then deformed with the indenter to a maximum load of 50 mN at a loading rate of 5 mN/s. While the indenter was maintained at that load, the temperature in the sample was brought to room temperature and then the indenter was withdrawn from the specimen. It took approximately 2 h for the sample to reach room temperature after the heater was turned off (Fig. 5). The surfaces of the specimens were then examined with a Wyko Optical Surface Profiler (Veeco Instruments, Inc.) for the initial indentation profile and indentation depth measurements. Subsequently, the specimen was placed back on the indenter microheater stage for recovery experiments. The recovery experiments were conducted at various temperatures ($T_r$): 60 °C, 75 °C, 93 °C, 98 °C, and 125 °C. A 2-minute recovery time was used for all experiments. The indentation profile at each recovery temperature was next obtained by scanning the surface of the recovered specimen with the optical surface profiler.

### 2.5. Dynamic mechanical tests

The thermomechanical behavior of the SMP in bulk form was characterized with a dynamic mechanical analyzer (DMA), Model Q800 from TA Instruments. Rectangular specimens, with nominal dimensions of 22 mm (length) × 15 mm (width) × 3.2 mm (thickness), were tested in torsion mode. Tests were scanned from 25 °C to 130 °C with a heating rate of 2 °C/min. The applied strain was 0.1% and the oscillating frequency was 1 Hz.

## 3. Results and discussion

### 3.1. Load-displacement and modulus

The present SMP is a two-part, fully formable thermoset resin system. At room temperature, the material is a rigid plastic. The room temperature load–depth response of the present SMP was examined with a spherical indenter, as shown in Fig. 6. The indenter loading/unloading rate was approximately 3.5 mN/s with a peak holding time of 10 s. For comparison, the analytical loading response based on Hertz is also included. The elastic deformation at small indentation is described by Hertz [27]

$$F = \frac{2\sqrt{2}}{3}\left(\frac{E\sqrt{2R}}{1-\nu^2}\right)h^{3/2} \tag{1}$$

where $R$ is the radius of the spherical indenter, and $E$ and $\nu$ are the modulus and Poisson ratio of the material, respectively. A Poisson's ratio value of 0.35 was used for the current SMP.

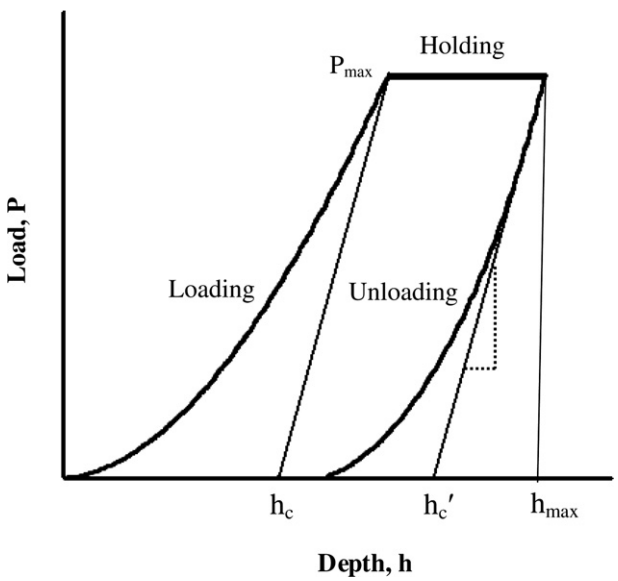


**Fig. 4.** Diagrammatic representation showing the "hold-at-the-peak" method used for nanoindentation of viscoelastic materials.

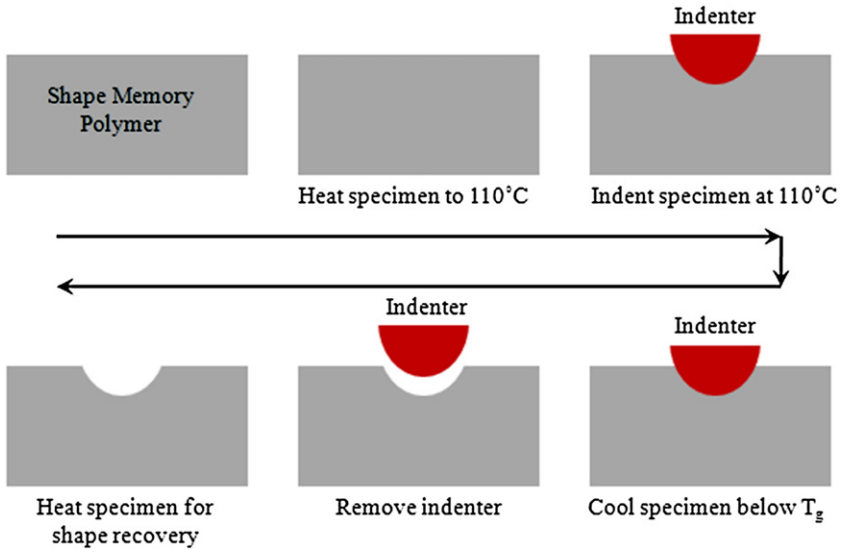


**Fig. 5.** Schematic of the present shape recovery experiment through high-temperature indentation.

It is seen that the initial loading response is mostly elastic, and is in relatively good agreement with the Hertzian theory for the ratio of the indentation depth to the diameter of the indenter up to 0.5. As the load increases, the experimental measurement deviates from the analytical prediction, due in part to the inelastic responses in the SMP. It has been reported that SMP in compression mode often exhibit elastic–plastic deformation at ambient condition [28]. In addition, viscous creep deformation is also observed in the present SMP during the indenter holding period, as shown in the inset in Fig. 6.

The nanoindentation tests were then performed on the SMP specimens over a range of temperatures, below and above $T_g$ (the present SMP has a $T_g$ of 105 °C as determined from the tan $\delta$ curve measured from DMA). Fig. 7 shows the resultant indentation load–depth responses using a loading/unloading rate of approximately 3.5 mN/s with a peak holding time of 10 s. As expected, the load–depth curve becomes less stiff as the temperature increases, since the material changes its state from a rigid plastic to a soft rubber. The viscous creep is clearly evident during the indenter holding period on each load–depth curve and is observed to accelerate substantially as temperature increases (Fig. 8). This creep displacement needs to be subtracted from the elastic contact depth formula. In addition, the contact depth between the indenter and the specimen depends upon the indenter holding time and unloading rate. After taking these factors into account, the elastic contact depth ($h_c$) during the indentation of a viscoelastic material is determined as follows [20]

$$h_c = (h_{max} - h_{creep}) - 0.75P_{max}\left(\frac{1}{S} - \frac{\dot{h}_v}{\dot{P}}\right) \quad (2)$$

where $h_{max}$ is the maximum indentation depth, $h_{creep}$, is the change in the indentation depth during the holding

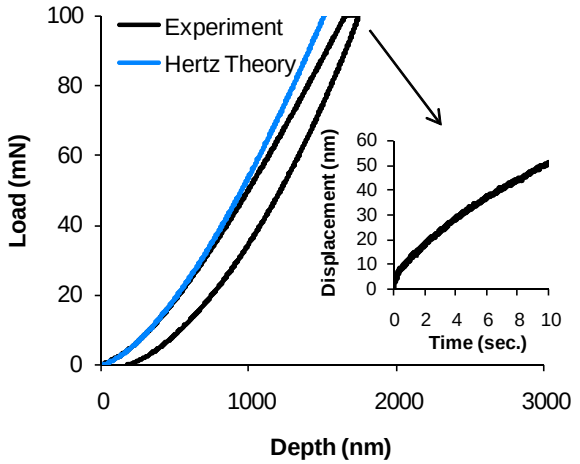


**Fig. 6.** Indentation load–depth responses of the SMP at room temperature.

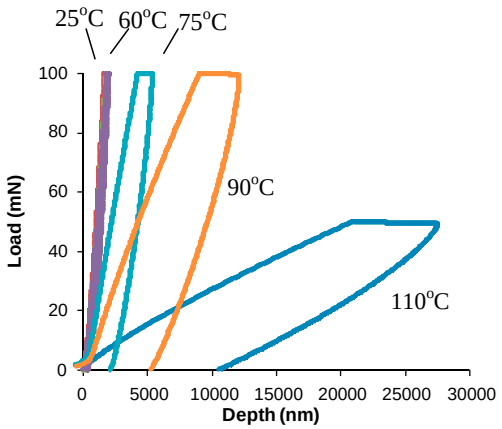


**Fig. 7.** Indentation load–depth responses of the SMP at various temperatures.

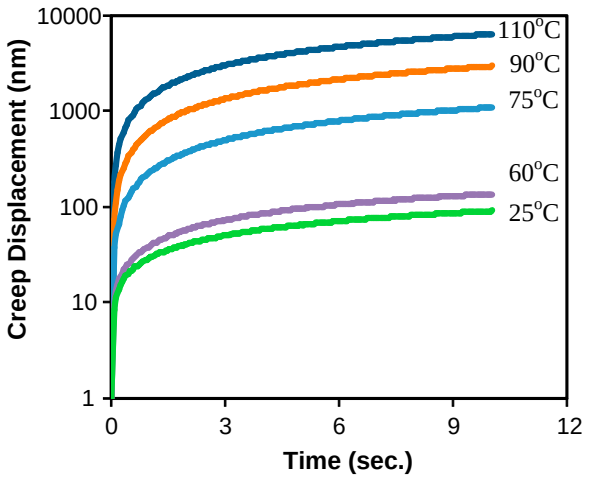


**Fig. 8.** Creep responses of the SMP occurred during indenter holding periods.

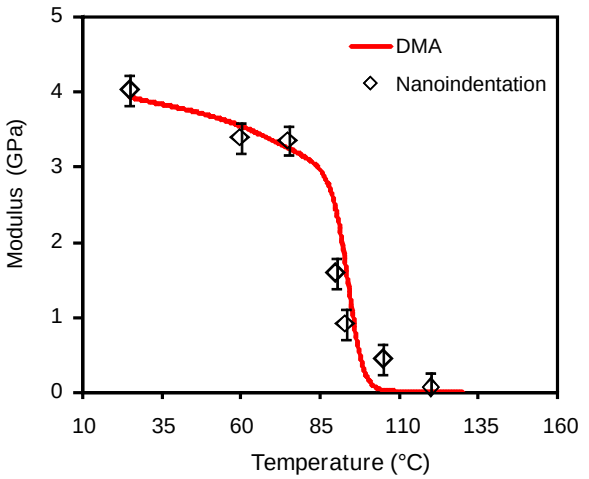


**Fig. 9.** Temperature-dependent moduli of the SMP measured from nanoindentation and dynamic mechanical analysis (DMA).

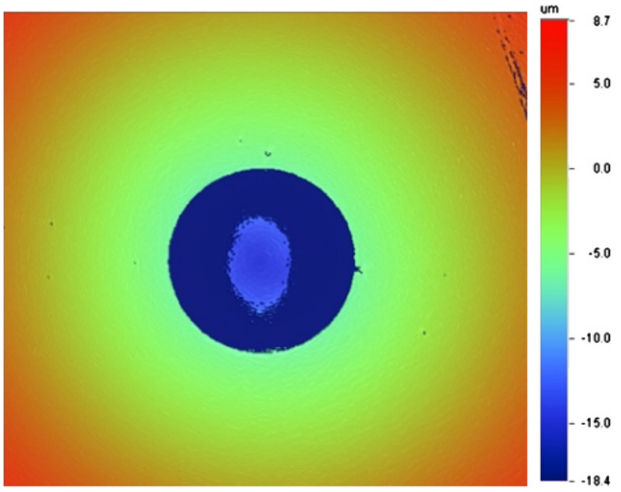


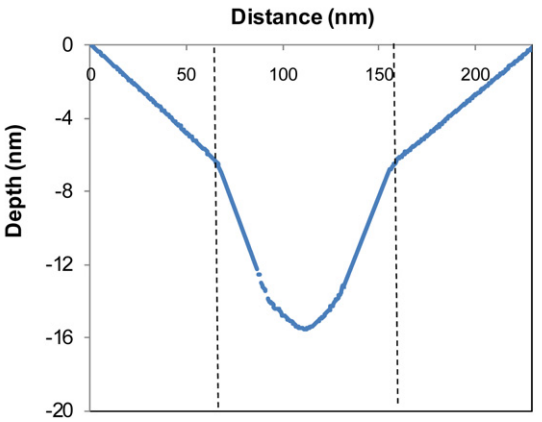


**Fig. 10.** Indentation profile of the SMP after activated above the glass transition temperature ($T_d = 110\ ^\circ C$).

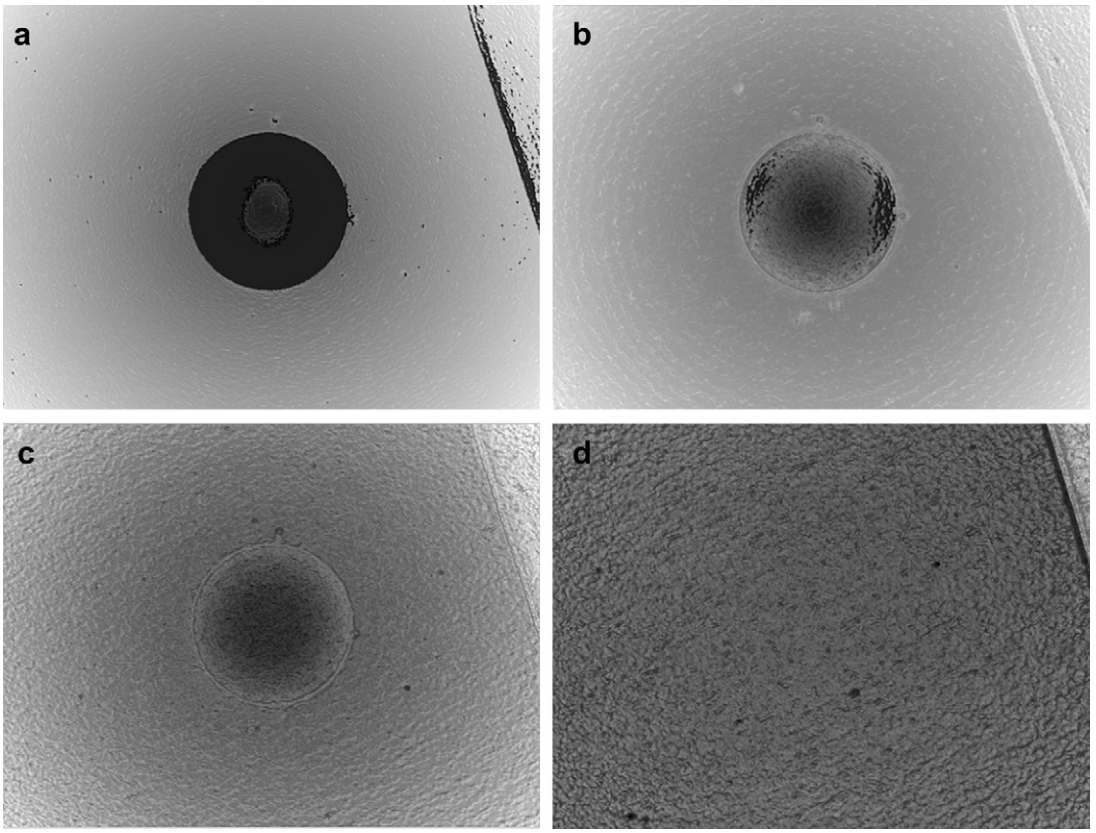


**Fig. 11.** Indentation surface of the SMP after each recovery experiment. The recovery temperatures are: (a) 75 °C, (b) 93 °C, (c) 98 °C, and (d) 125 °C.

time, $P_{max}$ is the peak load, $S$ is the elastic stiffness as determined from the slope of the unload curve evaluated at the maximum depth ($S = (dP/dh)_{h=h_{max}}$), $\dot{h}_v$ is the creep rate at the end of the load hold, and $\dot{P}$ is the indenter unloading rate.

The indenter-sample contact radius ($a$) is then computed via the standard procedure

$$a = \sqrt{2h_c R - h_c^2} \tag{3}$$

Once the elastic contact stiffness ($S$) and indenter-sample contact radius ($a$) are known, the elastic modulus $E$ of the testing sample can be calculated following the standard Oliver–Pharr procedure [22,23]

$$E = \frac{1-\nu^2}{\dfrac{1}{E_r} - \dfrac{1-\nu_i^2}{E_i}} \tag{4}$$

where $E_r = (\sqrt{\pi}/2 \cdot (1.034))(S/\sqrt{\pi a^2})$. $E_i$ and $\nu_i$ are the elastic modulus and Poisson's ratio of the indenter (for diamond indenter: $E_i = 1140$ GPa and $\nu = 0.07$).

The elastic moduli of the SMP at various temperatures ($T_r$) were calculated by using Equation (4), as shown in Fig. 9. Also shown in the figure is the storage modulus $E'$ obtained from dynamic mechanical analysis (DMA), where bulk SMP was tested in torsion mode. Overall, the modulus measured from indentation follows the same trend as that from the DMA. The mechanical behavior of the SMP is clearly divided into three distinctive regions: (1) a glassy region as $T < 85$ °C, (2) a transition region as 85 °C $< T <$ 105 °C and (3) a rubbery region as $T >$ 105 °C.

### 3.2. Shape recovery ability

The shape memory effect in glassy polymers is believed to be the result of rearrangement of long molecular chains as the material is cooled following deformation at elevated temperatures. During the cooling process, new bonds are developed between molecular chains and a fixed shape is achieved. Therefore, to properly characterize the shape memory effect, the material needs to be activated in its rubbery state at a deformation temperature above $T_g$. Recently, there has been increased interest in examining the shape memory effect of SMP on a small scale, as driven by the potential applications of SMP in micro-/nano-scale systems and devices [9,13–15]. In those studies, the shape memory behaviors have been mostly evaluated by using the micro/nanoindentation technique. However, the indentation deformations have been executed at ambient condition, i.e., the deformation temperature ($T_d$) is ambient temperature, which is below the glass transition temperatures of most thermoset SMP.

In the present study, the shape recovery of the SMP was examined using a high-temperature indentation technique,

as discussed earlier. Fig. 9 shows the indentation profile after the SMP was activated at elevated temperature ($T_d > T_g$), with the dashed vertical lines showing the indenter–specimen contact area. It is seen that the deformation zone has extended beyond the indenter–specimen contact. The indentation profile shows that the surface of the specimen has been substantially deformed. This indicates that there is a large amount of "sink-in" when indenting the SMP above its glass transition temperature. As $T_d > T_g$, the SMP is in a rubbery state and the deformation mechanism is mostly elastic. The large deformation at the sample surface is in sharp contrast with the observations obtained from room temperature indentation [9,13–15]. At low temperatures, the SMP is a rather rigid material and exhibits elastic–plastic type deformation. As a result, pile-up, rather than sink-in, has been often observed around the indentation. This kind of permanent deformation could be non-recoverable during subsequent heating, particularly at higher levels of stress/strain.

When activated at high deformation temperatures, the SMP can undergo a fairly large deformation (as shown from the indentation depth responses in Fig. 7), which is often required for applications involving morphing deployable structures. The indentation strain under a spherical indenter can be generally approximated as $\varepsilon_{ind} = 0.2 \cdot a/R$, where $a$ is the indenter–sample contact radius and $R$ is the indenter radius. For the present SMP that was activated at 110 °C, $a$ is estimated at approximately 95.6 μm (based on the indentation profile, Fig. 10), which corresponds to an indentation strain of 20%.

When the deformed SMP was re-heated to elevated temperatures (60 °C, 75 °C, 93 °C, 98 °C, and 125 °C), the indentation deformation starts to recover, as evidenced by the changes in indentation depth (Figs. 11 and 12). The indentation strain was calculated at each recovery temperature and used to evaluate the shape recovery of the SMP (Fig. 13). It is seen that the overall recovery process follows a trend similar to the modulus measurements obtained using DMA, as shown in Fig. 8. The indent recovery is small when the material is in the glassy state

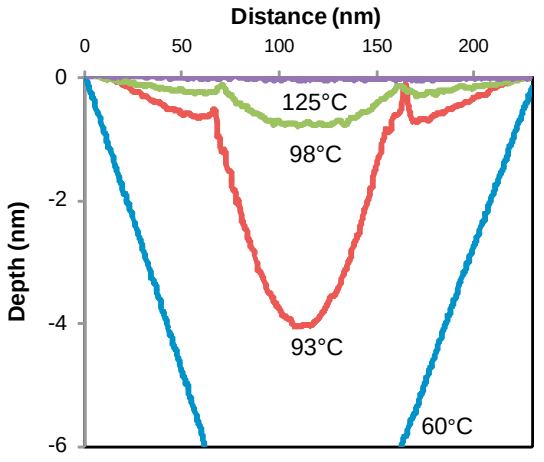


**Fig. 12.** Surface profiles of the SMP obtained at various recovery temperatures.

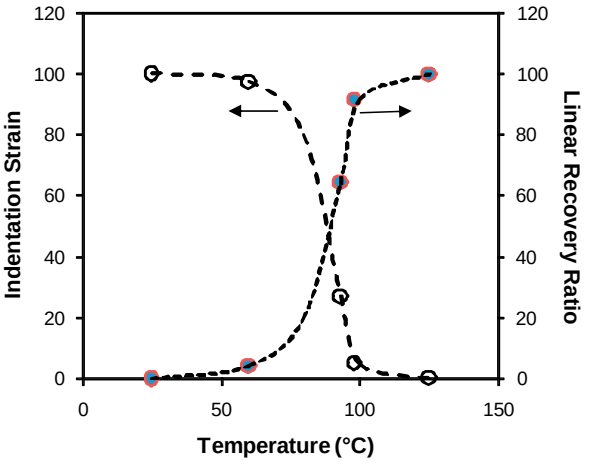


**Fig. 13.** Temperature-dependent indentation strain and shape recovery ratio of the SMP after activated with a high temperature nanoindenter.

(60 °C, 75 °C) and then increases in the transition state (93 °C, 98 °C). As the material was re-heated above its glass transition temperature (125 °C), the indentation strain has reduced to approximately 0.4%.

The shape recovery ability can also be characterized by the concept of linear shape recovery ratio, $R$ [29]. For the indentation experiments, $R$ can be defined as follows

$$R = (1 - h_f/h_i) * 100 \quad (5)$$

where $h_f$ is the final indentation depth corresponding to each recovery temperature and $h_i$ is the initial indentation depth. The variation of shape recovery ratio as a function of temperature is also shown in Fig. 13. The overall trend is in agreement with the change in indentation strain. As the temperature reaches the rubbery state ($T_r > T_g$), the material has a shape recovery ratio of 99%, indicating that the material has almost completely recovered.

## 4. Conclusions

The thermomechanical behavior of a thermosetting shape memory polymer (SMP) has been examined by using a high temperature nanoindentation technique. The thermal stability of the indenter frame has been verified by testing standard reference material. The load–depth curves of the SMP at various temperatures are obtained, from which the instantaneous moduli are calculated using a revised contact–depth formula. The temperature-dependent modulus of the SMP measured from nanoindentation follows the same trend as that from dynamic mechanical analysis on bulk samples. The micro-heater attached to the indenter sample holder allows the activations of the SMP at temperatures above its glass transition ($T_g$). The SMP activated at elevated temperatures exhibits a surface profile different from those activated at room temperature. When activated at elevated temperatures, the SMP surface has a large amount of "sink-in", an indication of large-strain elastic deformation. This large elastic deformation is fully recoverable when recovery takes place

at a temperature above the material's glass transition temperature.

## Acknowledgements

This work was partially supported by the American Society of Engineering Education – Air Force Summer Faculty Fellowship Program (SFFP) and by the grants from NASA EPSCoR Research Infrastructure Development (RID) Program and Kentucky Space Grant Consortium (KSGC).

## References

[1] A. Lendlein, S. Kelch, Shape-memory polymers. Angew Chem. Int. Ed. 41 (2002) 2034–2057.
[2] V.A. Beloshenko, V.N. Varyukhin, Y.V. Voznyak, The shape memory effect in polymers. Russ. Chem. Rev. 74 (3) (2005) 265–283.
[3] C. Liu, H. Qin, P.T. Mather, Review of progress in shape-memory polymers. J. Mater. Chem. 17 (16) (2007) 1543–1558.
[4] Y. Liu, K. Gall, M.L. Dunn, A.R. Greenberg, J. Diani, Thermomechanics of shape memory polymers: uniaxial experiments and constitutive modeling. Int. J. Plast. 22 (2006) 279–313.
[5] M. Behl, A. Lendlein, Shape-memory polymers. Mater. Today 10 (4) (2007) 20–28.
[6] D. Ratna, J. Karger-Kocsis, Recent advances in shape memory polymers and composites: a review. J. Mater. Sci. 43 (2008) 254–269.
[7] Z.G. Wei, R. Sandstrom, S. Miyazaki, Review shape-memory materials and hybrid composites for smart systems, part I shape-memory materials. J. Mater. Sci. 33 (1998) 3743–3762.
[8] C. Schmidt, K. Neuking, G. Eggeler, Functional fatigue of shape memory polymers. Adv. Eng. Mater. 10 (10) (2008) 922–927.
[9] K. Gall, P. Kreiner, D. Turner, M. Hilse, Shape-memory polymers for microelectromechanical systems. J. Microelectromech. Syst. 13 (3) (2004) 472–483.
[10] H. Tobushi, H. Hara, E. Yamada, S. Hayashi, Thermomechanical properties in a thin film of shape memory polymer of polyurethane series. Smart Mater. Struct. 5 (1996) 483–491.
[11] H. Tobushi, T. Hashimoto, N. Ito, S. Hayashi, E. Yamada, Shape fixity and shape recovery in a film of shape memory polymer of polyurethane series. J. Intell. Mater. Syst. Struct. 9 (1998) 127–136.
[12] B. Atli, F. Gandhi, G. Karst, Thermomechanical characterization of shape memory polymers. J. Intell. Mater. Syst. Struct. 20 (1) (2009) 87–95.
[13] B.A. Nelson, W.P. King, Shape recovery of nanoindentation imprints in a thermoset "shape memory" polymer. Appl. Phys. Lett. 86 (2005) 103108.
[14] E. Wornyo, K. Gall, F. Yang, W.P. King, Nanoindentation of shape memory polymer networks. Polymer 48 (11, 21) (2007) 3213–3225.
[15] F. Yang, E. Wornyo, K. Gall, W.P. King, Thermomechanical formulation and recovery of nanoindentation in a shape memory polymer studied using a heated tip. Scanning 30 (2008) 197–202.
[16] C.A. Schuh, C.E. Packard, A.C. Lund, Nanoindentation and contact-mode imaging at high temperatures. J. Mater. Res. 21 (2006) 725–736.
[17] B.D. Beake, J.F. Smith, High-temperature nanoindentation testing of fused silica and other materials. Philosophy Magazine A82 (2002) 2179.
[18] A.A. Volinsky, N.R. Moody, W.W. Gerberich, Nanoindentation of Au and Pt/Cu thin films at elevated temperatures. J. Mater. Res. 19 (9) (2004) 2650–2657.
[19] A. Sawant, S. Tin, High temperature nanoindentation of a re-bearing single crystal Ni-base superalloy. Scr. Mater. 58 (2008) 275–278.
[20] Y.C. Lu, D.C. Jones, G.P. Tandon, S. Putthanarat, G.A. Schoeppner, High temperature nanoindentation of PMR-15 polyimide. Exp. Mech. (2009). doi:10.1007/s11340-009-9254-5.
[21] CRG Industries, LLC, Dayton, OH, 2009. Available at: <http://crgindustries.com/product_data.htm>.
[22] W.C. Oliver, G.M. Pharr, An improved technique for determining hardness and elastic modulus using load and displacement sensing indentation experiments. J. Mater. Res. 7 (1992) 1564.
[23] W.C. Oliver, G.M. Pharr, Measurement of hardness and elastic modulus by instrumented indentation: advances in understanding and refinements to methodology. J. Mater. Res. 19 (2004) 3–20.
[24] A.H.W. Ngan, B. Tang, Viscoelastic effects during unloading in depth-sensing indentation. J. Mater. Res. 17 (10) (2004) 2604–2610.
[25] B.J. Briscoe, L. Fiori, E. Pelillo, Nano-indentation of polymeric surfaces. J. Phys. D. Appl. Phys. 31 (1998) 2395–2405.
[26] Y.T. Cheng, C.M. Cheng, Relationships between initial unloading slope, contact depth, and mechanical properties for conical indentation in linear viscoelastic solids. J. Mater. Res. 20 (4) (2005) 1046–1052.
[27] H. Hertz, in: H. Hartz, et al. (Eds.), Miscellaneous papers, Macmillan, London, 1863.
[28] H.J. Qi, T.D. Nguyen, F. Castroa, C.M. Yakackia, R. Shandas, Finite deformation thermo-mechanical behavior of thermally induced shape memory polymers. J. Mech. Phys. Solids 56 (2008) 1730–1751.
[29] G.P. Tandon, K. Goecke, K. Cable, J. Baur, Durability assessment of styrene- and epoxy-based shape memory polymer resins. J. Intell. Mater. Syst. Struct. 20 (2009) 2127–2143.